

Indistinguishable sub-nanosecond Pulse Generator

Pranshu Maan*
Robert Bosch GmbH
(Dated: May 4, 2022)

Indistinguishable laser pulse is important in realization of qubits in quantum cryptography. Implementation of such cryptography in automotive framework needs to be compact and cheap. However, modern implementation of quantum cryptography is bulky and expensive. Significant effort has been put into to reduce the form factor of quantum cryptography implementation. We report a compact, low cost, indistinguishable, sub-nanosecond pulse generator with adjusted delay and amplitude using a Fabry-Perot laser diode. The approach was derived based on algebraic topology formulation of electrical network, and the implementation is time dependent perturbation of a constant current node, generating tunable, sub-nanosecond excitation with constant pre-bias. Parameters for simulation model for the laser diode was obtained considering effect of spontaneous emission and relaxation oscillation. Typical measured FWHM of the pulse was 520ps, for operating frequency of 100KHz. The shortest pulse was measured to have FWHM of 496ps.

I. INTRODUCTION

Generation of indistinguishable excitation pulses are one of the fundamental requirements in many quantum information related experiments such as: indistinguishable pulses for quantum cryptography application[1][2][3], photon number resolution using APDs[4]. State of art implementations for these are either expensive or too bulky to fit in automotive gateway modules and controllers. This calls for further reduction in form factor and cost.

Different methods have been reported towards implementing quantum cryptography, namely: electro-optic modulators in photonic ICs, driver controlled variable attenuators. In 2015, Wabnig et al. at Nokia labs[9], proposed Quantum Key Distribution(QKD) based scheme using spatial filter to generate indistinguishable pulses, with Laser diode or LED. The indistinguishable pulses were defined by characteristics of the spatial filter. In 2016, in order to make QKD system compact, Bunnadar et al. at MIT[10], proposed photonic integrated chip to realize transmitter and receiver. These photonic ICs comprised of ring resonators. Corresponding to each of these resonators there were modulators that were capable of applying delay to optical pulses. Further, in 2017, Nordholt et al. at Los Alamos National Security[11], proposed another photonic integrated IC based approach. In this, a variable optical attenuator or amplitude modulator was used to reduce average number of photon per pulse. Similarly, in 2017, Yuan et al. at Toshiba[12], created a quantum communication system using variable attenuator to change intensity of the emitted laser pulses. These approaches often require complex and expensive driving circuits for variable optical attenuators. Direct modulation of laser is another preferred technique to generate indistinguishable excitation[5], as mean number of photon in each pulses can be reduced to less than 1 using a constant optical attenuator, without engendering

need of using dedicated driver circuit for the attenuator. However, the state of art was massive, pulse duration obtained was in nanosecond range and pulse characteristics were not adjustable.

In this paper, inspired by algebraic topology, we show by simulation and experimental measurement, generation of tunable, indistinguishable, sub-nanosecond excitation. We have achieved shortest injection current FWHM of 496ps using direct modulation of the laser diode. We further show, using simulation, excitation pulse can be tuned to exactly match characteristics in temporal domain. Implementation of quantum cryptography has proven challenging in terms of cost, form factor and integration into existing infrastructure. This approach can provide low cost and small form factor implementation of quantum cryptography transmitter (and receiver) with greater integration into existing automotive framework.

II. THEORY

Let us visit some preliminaries pertaining to chain complexes:

Definition II.1 (Boundary operator ∂). : If ∂_n is a boundary operator that is a linear transformation on sequence of vector space C_n as $\partial_n : C_n \rightarrow C_{n-1}$, we write:

$$C_n \xrightarrow{\partial_n} C_{n-1} \xrightarrow{\partial_{n-1}} C_{n-2} \dots \xrightarrow{\partial_2} C_1 \xrightarrow{\partial_1} C_0 \xrightarrow{\partial_0} 0$$

a chain complex if $\partial_n \cdot \partial_{n+1} = 0$. If boundary operator on a branch ω is defined as: $\partial\omega = \Omega(e-s)$ where e is the end node and s is the start node of branch Ω , then we can interpret the first operator ∂_n on 1-chain complex as nodes. Since node does not have boundary, second boundary operator on the node, ∂_{n+1} , is zero.

We can now define kernel of a boundary operator.

Definition II.2. If a k-chain has no boundary, then it is called k-cycles and can be represented as a kernel of

* Pranshu.Maan@us.bosch.com

the boundary operator[6]:

$$Z_1 = \ker \partial k \quad (1)$$

if $k \in Z_1$

$$\partial k = 0 \quad (2)$$

Lemma II.1. Boundary for branches can be expressed as a sum of all the branches that leave and enter a node.

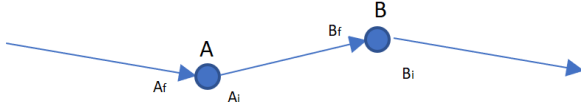


Figure 1. Definition of boundary operator of a branch $|A_f$ is the branch with A as final node $|A_i$ is the branch with A as initial node $|B_f$ is the branch with B as final node. Similarly, B_i is the branch with B as initial node.

Proof. Fig. 1 represents node A and node B, where A_f and A_i are branches with node A as final and initial node respectively. Similarly, B_f and B_i are branches with B as final and initial node respectively. If $K \in C_1$ is a set of all branches such that

$$\partial K = \{k_a, k_b \dots\} \quad (3)$$

Here $k_i \in C_0$ represents branches that enter and leave node i and can be represented as

$$k_i = k_{ei} - k_{li} \quad (4)$$

where k_{ei} and k_{li} represent branches that enter and leave node i respectively, irrespective whether it is time-independent or not.

With reference to Fig.1:

$$\partial K = A_f(A - \Delta_i) + B_f(B - A) \quad (5)$$

where Δ_i represents arbitrary start node of the branch A_f . Consolidating all the terms pertaining to node A together:

$$\partial K = A(A_f - B_f) + B(B_f) - \Delta_i(A_f) \quad (6)$$

The first term in eqn. 6 pertains to node A, represents branch entering the node (-) branch leaving the node, and it is valid for both constant as well as time dependent branches. \square

Consider an electrical sub-network represented by $\{N, B, \partial, R_{dc}, R_{perturbation}\}$, where branch $B \in C_1$ one chain vector space and node $N \in C_0$ zero chain vector

space, $\partial : C_1 \rightarrow C_0$ is the boundary map, R_{dc} is the coefficient ring for dc excitation and $R_{perturbation}$ represents coefficient ring for time dependent perturbation on node Δ . If Z_1 represents kernel of boundary map, then:

$$I \in Z_1 \quad (7)$$

$$\partial I = 0 \quad (8)$$

$$\partial I = I_{\delta_\alpha} - (I_{\delta_\beta} + I_{\delta_\psi}) = 0 \quad (9)$$

$$I_{\delta_\psi} = I_{\delta_\alpha} + I_{\delta_\Delta} \quad (10)$$

where branches that enters or leaves the node Δ , $\delta_i \in C_0$, $\delta_\beta = -\delta_\Delta$ is the time dependent negative perturbation applied on node β and δ_α is the constant excitation on node α .

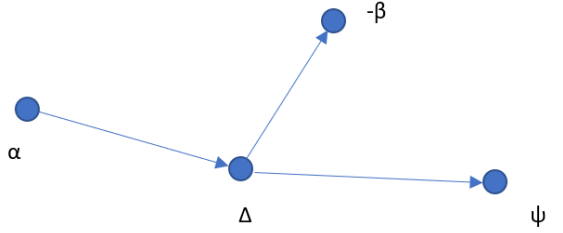


Figure 2. Electrical sub-network for generation of excitation pulse $|\Delta$ is the constant current node, β is the negative perturbation node, α is the constant excitation node, ψ is the output node | Laser diode (or APD for voltage perturbation) is connected at ψ node

Here eqn. 10 can be interpreted as a time dependent perturbation current on node ψ with certain pre-bias current.

In a laser diode, when injection current is low, spontaneous emission due to carrier relaxation dominates and photon emission varies slowly as a function of injected current. Once injected current approaches threshold region, steady state injected current approaches a constant value i.e. spontaneous emission is nearly constant and stimulated emission dominates. This emission in dominant mode is linearly dependent on injection current and each injected carrier results in a photon. Further, relation between resulting injected carrier density and optical intensity can be derived based on laser rate equation for single resonator mode and can be modelled in terms of resistors, capacitors and inductors. Value of these RLC components can be calculated in terms of electron density and photon density[7]. In addition, contribution of spontaneous emission and relaxation oscillation can be also expressed in terms of electrical parameters and electron, photon density[7].

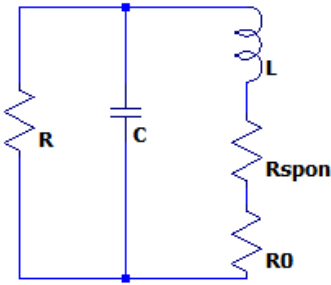


Figure 3. Equivalent circuit model for laser diode[7] | $R = 2.555\Omega$, $L = 6.184\text{pH}$, $C = 0.3557\text{nF}$, $R_{se} = 2.811\text{m}\Omega$, $R_o = 5.511\text{m}\Omega$

$$R = \frac{R_d}{n_{photon} + 1} \quad (11)$$

$$L = \frac{R_d \tau_{photon}}{n_{photon}} \quad (12)$$

$$C = \frac{\tau_{spon}}{R_d} \quad (13)$$

$$R_{spon} = \frac{\beta R_d n_e}{n_{photon}^2} \quad (14)$$

$$R_o = \frac{-R_d \delta}{n_{sat}} \frac{1}{[1 + \frac{n_{photon}}{n_{sat}}]^2} \quad (15)$$

where $R_d = \frac{2kT}{q} \frac{1}{I_d}$ is called differential resistance of the laser diode, n_{photon} , τ_{photon} , τ_{spon} are photon density, lifetime of photon and spontaneous emission rate of electrons respectively. R_{sat} represents photon saturation density and β represents amount of spontaneous emission that couples into cavity mode of the laser diode. All the circuit components (inductor, resistance due to spontaneous emission and relaxation oscillation) related to optical phenomenon appears in series, as expected from laser rate equation. Differential resistance decreases with injection current, when below the threshold, and remains nearly constant when injected current is above the threshold.

III. SIMULATION

In this section, we discuss simulation model for analyzing current injection profile into the laser diode. Additionally, using the simulation, we show delay and amplitude tuning of the sub-nanosecond perturbation.

Fig. 4 represents of simulation model for generating indistinguishable excitation pulse. Shape tuning module comprises of a circuit capable of generating any arbitrary shape excitation. Shape and frequency of the excitation determines frequency and initial characteristics of each perturbation pulse. Shape controlled excitation acts as an input for OPAMP and logic network block. The block comprises of operational amplifier and Logical network to implement complimentary output detector through a tunable differential delay generator. Tun-ability of the block further provides selection of wide range of pulse-width, amplitude and delay for the excitation to generate time-dependent perturbation. Constant node, α from Fig. 2, in the design is excited by a trans-conductance amplifier. Output node ψ is a time dependent perturbation with some pre-bias current as per eqn.10. This excitation node then drives a laser diode. When driving an APD, similar concept can be used to generate tuned voltage excitation. Design of these blocks are determined by magnitude of current/voltage and timing requirements. OPAMP and Logic block was designed to generate perturbation of upto 25mA of peak current. Had this requirement been higher, an additional driver stage would then be required.

Simulation model for the laser diode was obtained based on discussion in section II. It comprises of a parallel capacitor which arises due to carrier relaxation, differential resistance arising due to carrier injection, and inductance due to photon emission. Additional resistances are due to spontaneous emission and relaxation oscillation in the laser diode (Fig. 3). Values for laser diode simulation model were obtained for a laser diode with threshold current value of 18.4mA, at room temperature, and following parameters were considered: $R = 2.555\Omega$, $L = 6.184\text{pH}$, $C = 0.3557\text{nF}$, $R_{spon} = 2.811\Omega$, $R_o = -5.511\text{m}\Omega$.

In addition, a filter stage is designed based on magnitude of attenuation required for filtering of the excitation pulse. Moreover, this stage can also provide feedback for control circuitry in the implementation.

Fig.5 shows time dependent negative perturbation of around 7.5mA generated at the constant current node, which corresponds to node Δ in Fig.1. The negative perturbation at β is applied at the constant current node Δ by OPAMP and Logic block through a bias tee network.

Fig.6 represents excitation current into the laser diode connected at the output node ψ in Fig.1. The baseline current of 31mA represents constant current excitation from node α . Fig.7 represents zoomed in version of excitation shown in Fig.6. Sub-nanosecond pulse of FWHM 600ps can be observed. Simulation model does not completely consider parasitic effect of the PCB as operating frequency is 100KHz. In addition, any deviation in IC from the model considered for simulation will have impact on the observed pulse characteristics. Fig.8 represents tunability achieved in the laser excitation. Excitation delay was tuned by approximately 8ns (red and blue). Moreover, amplitude of the pulse was tuned from 41.5mA to

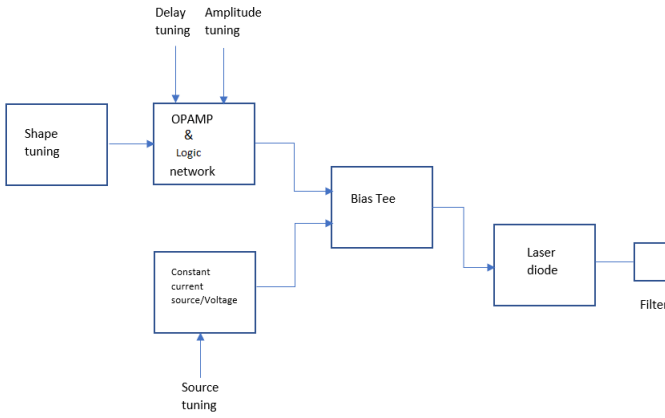


Figure 4. *Simulation block diagram | model can be adapted for APD instead of a laser diode | shape tuning circuit generates square, ramp or any arbitrary shape, OPAMP Logic network is a network comprising of operational amplifiers and FETs (can also be a digital IC) to generate tuned perturbation | Filter is used to further suppress any relaxation oscillation*

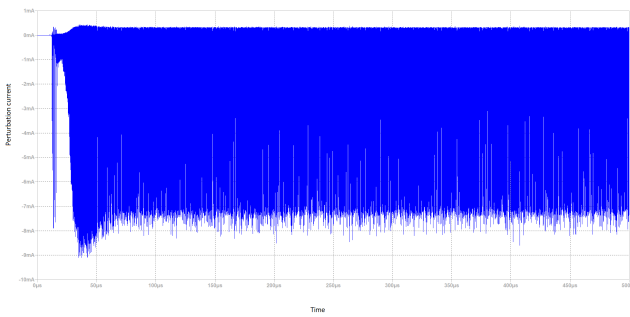


Figure 5. *Simulated negative perturbation applied at node β | the plot shows multiple sub-nanosecond perturbation*

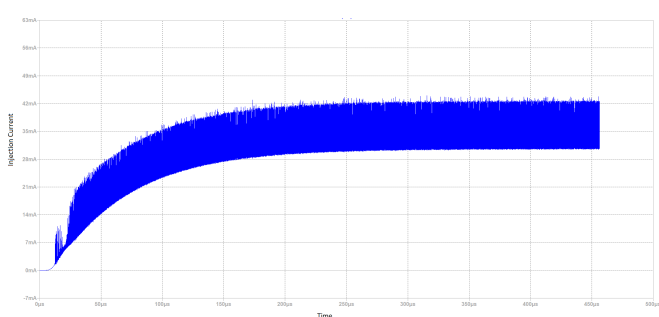


Figure 6. *Simulated current excitation profile at node ψ | The plot shows sub-nanosecond perturbation on a constant excitation of 31mA*

39.2mA. Amplitude tuning can also be achieved by adjusting the constant excitation applied at node α .

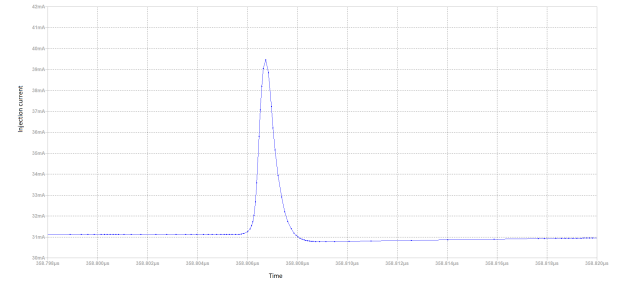


Figure 7. *Simulated sub-nanosecond pulse excitation as seen on node ψ | The plot is zoomed in version of Fig.6*

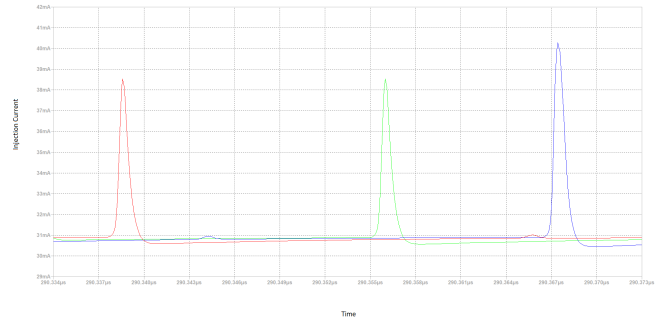


Figure 8. *Simulation of tunability in pulsed excitation | The parameter was obtained by varying one of the controlled parameters. Plot in red and green demonstrate tunability in delay and plot in blue represents tunability in amplitude of the perturbation. Amplitude tuning can also be achieved by tuning the constant current excitation, which represents shifting the base current*

IV. EXPERIMENT AND RESULTS

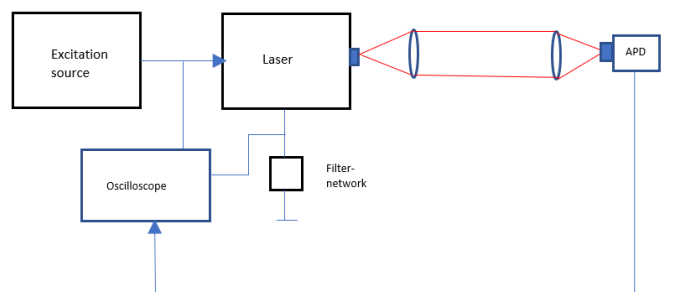


Figure 9. *Experimental setup for estimating current injection and output power of the laser diode | Excitation source represents node ψ . Differential current into the laser diode and APD, which detects focused laser (in red), is monitored using an oscilloscope*

Experiment was carried out to verify sub-nanosecond, indistinguishable pulse generation from the laser diode, by measuring differential voltage across its terminals us-

ing differential probe D420-A-PB with a 4GHz DX20-SI tip connected to 4GHz Lecroy 640Zi Waverunner. Profile of emitted optical pulses was estimated using an active probe ZS2500 with 2GHz bandwidth and a custom built SAP500 APD detector operating in linear region. Since our receiver SAP500 APD is bandwidth limited, it does not provide accurate estimation of actual pulse width of the sub-nanosecond optical pulse. However, the profile can be verified from profile of the excitation perturbation across the laser diode. Fig.9 represents schematic of the experimental setup. Excitation source with pre-biased, sub-nanosecond current perturbation drives HL6748MG, a 670nm laser diode (For cryptography application, it will be interesting to analyze coherence length and coherence time of this low cost diode). In addition, a filter is connected in series with the laser diode to sense current and for suppressing any oscillation. Also, feedback from the current sense can be used to track any change in temperature. For our application in automotive framework, we need extremely low cost implementation. Since the laser driver is driven near to the threshold region, and that the pulsed excitation is less than 1ns with frequency of 100KHz, average case temperature of laser diode will be near to the room temperature. This way temperature control will not be needed. Emission from the laser diode is monitored using custom made SAP500 based detector with the APD biased in linear region. The detector was selected based on efficiency corresponding to lasing wavelength of the laser diode. Fig.10 characterizes differential injection pulse through the laser diode. The shortest FWHM was observed to be 496ps. DC offset current due to pre-bias from the Fig.9 has been subtracted to underline pulse characteristics.

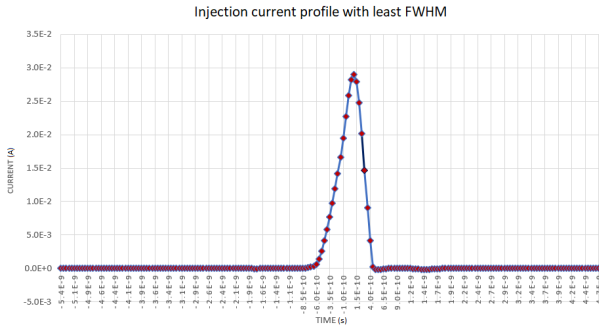


Figure 10. *Measured current excitation profile with least FWHM of 496ps | constant current excitation has been subtracted to underline pulse characteristics*

Fig.11 and Fig.12 represents indistinguishable current injection profile for pre-bias current above and below the threshold respectively. In these figures, noisy waveforms were averaged over 1000 samples.

Peak output power from the laser diode can be roughly estimated as follow from APD measurement: output peak current in the 50Ω at the APD terminal is around 10mA. Since the peak current further reduces applied bias, under constant excitation, we had voltage drop

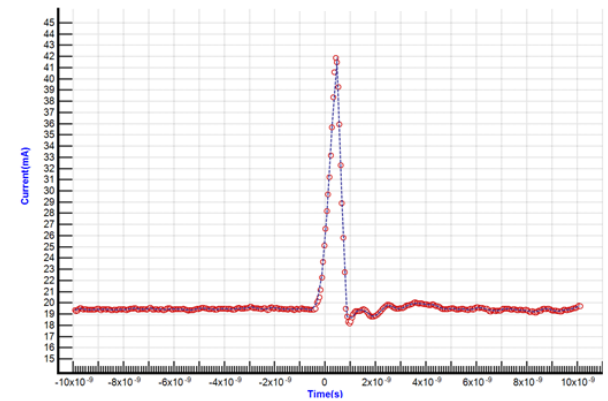


Figure 11. *Measured current injection profile for the laser diode with constant current excitation of approximately 19mA and perturbation of 23mA*

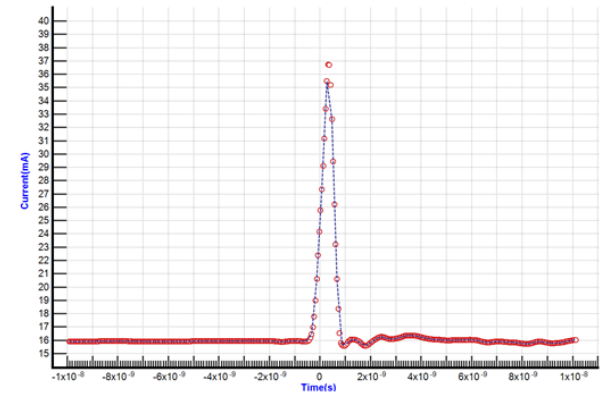


Figure 12. *Indistinguishable injection current with lower amplitude measured for the laser diode | lower amplitude can be achieved by tuning the perturbation or tuning the pre-bias current*

up to 100V across 50Ω resistor which corresponds to $200\mu A$ of continuous current into the APD, which is the maximum rating that should not be exceeded. Due to this peak current, there would be further drop in the applied bias. Ball-parking the effective applied bias of $<100V$ i.e around 30A/W for 670nm, even we consider 100% coupling efficiency and ball-parking the quantum efficiency at $<30\%$, we estimate peak output power of more than 1mW for excitation at 100KHz. In this estimation, emission due to perturbation pulse only is considered because emission due to pre-bias will be completely suppressed by a constant optical attenuator. Since, indistinguishability in terms of waveform shape is critical for our application, and so far we have considered indistinguishability in temporal domain. We have not considered any distinguishability in frequency domain due to chirps. It will be interesting to study impact on spectral indistinguishability using proposed approach.

V. CONCLUSION

We have designed a compact (4.5cmx3cm), sub-nanosecond, tunable-indistinguishable laser pulse generator with shortest FWHM measured around 496ps (Ideally, it will be less than 496ps if we consider contribution due to probe effect). Further, this can also be used to generate shape tunable excitation for active quenching of APD in single photon detection experiment, and to perform photon number resolution using APD. Indistinguishability in spectral domain, using this technique, should be explored.

VI. ACKNOWLEDGEMENT

This study is funded by Robert Bosch GmbH.

VII. REFERENCES

1. Yin, HL., Zhou, MG., Gu, J. et al. Tight security bounds for decoy-state quantum key distribution. *Sci Rep* 10, 14312 (2020). <https://doi.org/10.1038/s41598-020-71107-6>
2. Wei, Z., Wang, W., Zhang, Z. et al. Decoy-state quantum key distribution with biased basis choice. *Sci Rep* 3, 2453 (2013). <https://doi.org/10.1038/srep02453>
3. Decoy State Quantum Key Distribution, Lo et al. arXiv:quant-ph/0411004
4. Kardynal, B., Yuan, Z. Shields, A. An avalanche-photodiode-based photon-number-resolving detector. *Nature Photon* 2, 425–428 (2008). <https://doi.org/10.1038/nphoton.2008.101>
5. Richard A. Linke, Alan H. Gnauck, "High Speed Laser Driving Circuit And Gigabit Modulation Of Injection Lasers," Proc. SPIE 0425, Single Mode Optical Fibers, (8 November 1983); doi: 10.1117/12.936224
6. Smale, S.. "On the mathematical foundations of electrical circuit theory." *Journal of Differential Geometry* 7 (1972): 193-210.
7. J. Katz, S. Margalit, C. Harder, D. Wilt and A. Yariv, "The intrinsic electrical equivalent circuit of a laser diode," in *IEEE Journal of Quantum Electronics*, vol. 17, no. 1, pp. 4-7, January 1981, doi: 10.1109/JQE.1981.1070628.
8. Signal sources, conditioners and power circuitry, Jim Williams, November 2004
9. Joachin Wabnig et al. 2015 Secured Wireless Communication US 9,641,326,B2,(<https://patft.uspto.gov/netacgi/nph-Parser?Sect1=PT02&Sect2=H1OFF&p=1&u=%2Fnetacgi%2FPT0%2Fsearch-bool.html&r=1&f=G&l=50&co1=AND&d=PTXT&s1=wabnig.AANM.&OS=AANM/wabnig&RS=AANM/wabnig>)
10. Bunandar, Darius et al. 2016 Apparatus and methods for quantum key distribution, US10,158,481 B2, (<https://patft.uspto.gov/netacgi/nph-Parser?Sect1=PT02&Sect2=H1OFF&p=1&u=%2Fnetacgi%2FPT0%2Fsearch-adv.htm&r=25&f=G&l=50&d=PTXT&s1=bunandar&OS=bunandar&RS=bunandar>)
11. Nordholt et al. 2017, Quantum Communication system with integrated photonic devices. US 9, 819,418 B2, (https://worldwide.espacenet.com/publicationDetails/originalDocument?FT=D&date=20171114&DB=&locale=en_EP&CC=US&NR=9819418B2&KC=B2&ND=4#)
12. Yuan et al. 2017, Interference system and an interference method, US 9,696, 133 B2 (https://worldwide.espacenet.com/publicationDetails/originalDocument?FT=D&date=20170704&DB=&locale=en_EP&CC=US&NR=9696133B2&KC=B2&ND=4#)